Available online at www.sciencedirect.com
SCIENCE DIRECT®
Optics Communications 229 (2004) 29–37
OPTICS COMMUNICATIONS
www.elsevier.com/locate/optcom

Speckle interferometric technique to assess soap films

Myrian Tebaldi [a,*], Luciano Ángel [b], Néstor Bolognini [a,1], Marcelo Trivi [c,2]

[a] Centro de Investigaciones Ópticas, CIOp (CONICET, CIC) and OPTIMO (Dpto. Fisicomatemática, Facultad Ingeniería, UNLP), P.O.Box 124, Gonnet La Plata 1900, Argentina
[b] Departamento de Ciencias Básicas, Universidad EAFIT, Medellín, Colombia
[c] Instituto Nazionale di Ottica Applicata, Largo E. Fermi 6, 50125 Firenze, Italy

Received 4 June 2003; received in revised form 30 September 2003; accepted 17 October 2003

Abstract

An speckle interferometric technique to monitor the thinning process of vertical soap film before the film rupture is presented. The interferometric arrangement consists in a double aperture pupil optical system which images an input diffuser. In a first step, a reference specklegram is stored in the computer buffer memory. Afterwards, the soap film is located in front of one pupil aperture, an uniform displacement of the diffuser is produced and a new speckle pattern is stored. The soap film status is characterized in terms of the changes that this dynamic phase object introduces in the correlation fringes obtained by applying a FFT algorithm to the resulting summed specklegram. This procedure is done in real time as far as the soap film evolves in the successive status. It is experimentally demonstrated that the soap film during drawing acts as a variable wedge. The correlation fringes behavior becomes an important tool to establish the wedge shaped soap film angle and the thickness variations.

PACS: 42.30.Ms; 07.60.Ly

Keywords: Speckle interferometry; Soap film

1. Introduction

The color changes of a soap bubble due to progressive thinning of the liquid film at the surface of the bubble and the changes in the interference condition of the white light reflected by the film are well known. This phenomenon was first studied by Newton [1], who also observed black films. This type of film is reached in the last state of the thinning process, before the film rupture. This process is generally formed from solutions of an ionic surfactant in the presence of a salt.

Several techniques to study the thinning behavior on soap films were proposed [2–5]. The soap film is formed when pulling a frame out of a

* Corresponding author. Tel.: +54-221-4840280; fax: +54-221-4712771.
E-mail address: myrianc@ciop.unlp.edu.ar (M. Tebaldi).
[1] Also Facultad de Ciencias Exactas, UNLP, La Plata, Argentina.
[2] Present address: Centro de Investigaciones Ópticas, La Plata, Argentina.

0030-4018/$ - see front matter © 2003 Elsevier B.V. All rights reserved.
doi:10.1016/j.optcom.2003.10.021

reservoir with a surfactant solution. As a consequence of the drainage of the solution from the inner layer of the film, a thinning process takes place. The process is produced by the pressure difference between the film center and borders, caused by gravity, if the film is vertical and capillarity, acting in all cases. Indeed, the borders of the film are curved to adjust the contact angle requirements with the supporting frame [6]. The thickness evolution behavior as a function of time is used to obtain information on the nature and range of the intermolecular forces that are responsible for the film formation.

As it is well known, when an optically rough surface is illuminated by coherent light, speckles appear in front of the surface. Displacements and deformations of an input diffuser produce displacements and structural changes in the speckle patterns, which can be analyzed on the basis of the double-exposure imaged speckles, before and after deformation [7]. Some methods have been implemented on the basis of internal modulation of the speckle grains in the image field, which can be achieved by locating a double aperture pupil mask in front of the imaging lens [8]. In some applications, the number of apertures or the aperture shape of the optical system are modified between exposures [9,10].

Recently, we presented a novel speckle interferometer for phase object detection [11,12]. In [12], we theoretically analyzed the properties of a double-exposure specklegram generated through a double-aperture system, by assuming that a phase object is located in front of one of the apertures in one exposure. Besides, the pupil change is accompanied by a uniform in-plane displacement of the diffuser between exposures.

Several optical techniques have been used to visualize fluid flows and drawing. The phase variations associated with the fluid changes are displayed in the form of fringe patterns [13,14]. In the present paper, the speckle interferometric technique described in [12] is employed to characterize soap films evolution. The arrangement consists in a double aperture pupil optical system which images an input diffuser. In a first step, a reference specklegram is stored in the computer buffer memory. Afterwards, the soap film is located in front of one pupil aperture, a uniform displacement of the diffuser is produced and a new speckle pattern is stored. The soap film to be characterized is formed when pulling a frame out of a reservoir with a surfactant solution. A digital sum of a given status of the speckle pattern and the reference speckle is done. The soap film status could be determined in real time by applying a FFT algorithm to the resulting summed images and it is characterized in terms of the changes that this dynamic phase object introduces in the correlation fringes observed in the Fourier transform. As it is usual in optical techniques, the physical soap film parameters are encoded in the fringe patterns. Note that the experimental results confirm that the soap film behaves as a variable wedge in the drainage process and therefore the theoretical analysis of [12], whose results are presented in Section 2, suits very well to study this phenomenon. The changes in the peak position, frequency and orientation of the correlation fringes are utilized to determine the soap film behavior. The detailed procedure is done while the soap film evolves in the successive status. The correlation fringes behavior becomes an important tool to establish the wedge shaped soap film angle, the soap film thickness variation and whether the thicker part of the wedge is in the upper or lower region of the aperture. We demonstrate that the technique is very simple and accurate to measure the dynamic drawing of a surfactant solution.

2. Theoretical analysis

In [12], the properties of a double-exposed specklegram generated through a double-aperture pupil are analyzed. The write-in experimental arrangement is schematized in Fig. 1. A diffuser, which is placed in the input plane x–y, is illuminated by use of a collimated laser beam of wavelength λ and imaged onto the plane X–Y by lens L. Z_0 and Z_C denote the distance from the diffuser to the lens and from the lens to the image plane, respectively. A uniform in-plane displacement of the diffuser $(\Delta x^{12}, \Delta y^{12})$ occurs between exposures. Each aperture of the double aperture pupil mask is described by

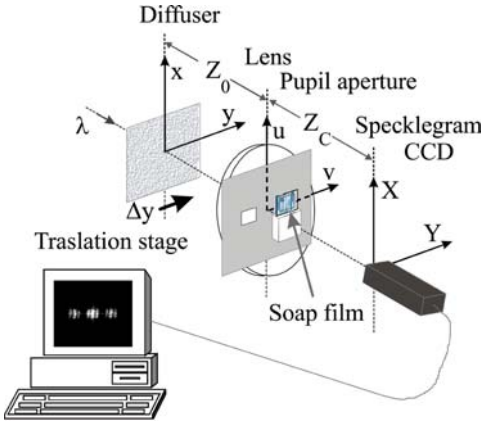

Fig. 1. Experimental set-up: $Z_0 = 138$ mm; $Z_C = 382$ mm; $D = 3.8$ mm; and $d = 10$ mm.

$$a(u-u_j, v-v_j) = \begin{cases} 1 & \text{inside the } j\text{th aperture} \\ 0 & \text{otherwise} \end{cases} \qquad j = 1, 2, \quad (1)$$

where the vector (u_j, v_j) determines the geometrical locus of the jth aperture. The function $a(u, v)$ describes the aperture shape.

Let us consider that the double aperture pupil remains fixed in both exposures, although a wedge-like phase object is located in front of the aperture $a(u-u_2, v-v_2)$ in the second exposure. In this case, the pupil associated to the second exposure can be written as

$$P(u,v) = a(u-u_1, v-v_1) + t\exp[i(\gamma+\tau u)] \times a(u-u_2, v-v_2), \quad (2)$$

where t and $\gamma + \tau u$ represent the amplitude transmission and the phase change the wedge introduces to the aperture $a(u-u_2, v-v_2)$. The parameters $t(0 \leqslant t \leqslant 1)$, γ and τ are real constants. In this case, the u-axis is perpendicular to the thin edge of the wedge. For square apertures of side D the aperture shape is $a(u,v) = \mathrm{rect}(u/D)\mathrm{rect}(v/D)$.

In the conditions described above, the speckle pattern is stored before and after the phase object introduction and a Fourier transform operation on the resulting summed speckle distribution is done. The theoretical smoothed intensity distributions obtained in the Fourier plane (U, V) for the zero and the (± 1) lateral diffracted orders result in [12]

$$\langle I^0(U,V)\rangle = K\,D^2\,T\left(\frac{\vartheta U}{D}\right)T\left(\frac{\vartheta V}{D}\right) \times \left\{3 + t^4 + 2\left[1 + t^4 + 2t^2\cos(\vartheta\tau U)\right]^{1/2} \times \cos\left[\frac{2\pi}{\lambda f}\left(U\Delta X^{12} + V\Delta Y^{12}\right) - \tan^{-1}\left[t^2\sin(\vartheta\tau U)/\left(1 + t^2\cos(\vartheta\tau U)\right)\right]\right]\right\}, \quad (3)$$

$$\langle I^{\pm 1}(U,V)\rangle = K\,D^2\,T\left(\frac{\vartheta U \mp u_{12}}{D}\right)T\left(\frac{\vartheta V \mp v_{12}}{D}\right) \times \left\{1 + t^2 + 2t\,\mathrm{sinc}\left[\frac{\tau D}{2\pi} \times \left(1 - \frac{\vartheta U \mp u_{12}}{D}\mathrm{sign}(\vartheta U \mp u_{12})\right)\right] \times \cos\left[\frac{2\pi}{\lambda f}\left(U\left(\Delta X^{12} - \frac{\lambda Z_C}{4\pi}\tau\right) + V\,\Delta Y^{12}\right) \mp \gamma \mp \frac{u_1+u_2}{2}\tau\right]\right\}, \quad (4)$$

where K is a proportionality factor, $\vartheta = Z_C/f$, $(u_{12}, v_{12}) \equiv (u_2 - u_1, v_2 - v_1)$, T is a triangular function, λ is the laser beam wavelength, f is the focal length of the Fourier transforming lens and $(\Delta X^{12}, \Delta Y^{12})$ is the relative displacement between the diffuser images. Note that $(\Delta X^{12}, \Delta Y^{12}) = -(Z_C/Z_0)(\Delta x^{12}, \Delta y^{12})$, where $(\Delta x^{12}, \Delta y^{12})$ is the diffuser displacement. The factor $-Z_C/Z_0$ represents the imaging magnification provided that the speckle displacement takes place near the optical axis.

A minute discussion of the meaning of Eqs. (3) and (4) was presented in [12]. It results from the analysis that if the diffuser in-plane displacement and the thin edge wedge are parallel, the fringes rotate when compared with the situation without the wedge. The fringe rotation increases as the value of the wedge parameter τ increases. It should be noted that the fringe visibility decreases when τ increases.

The previous analysis corresponds to the situation where the thin edge wedge and the image in

plane displacement direction are parallel. Note that any general diffuser displacement with respect to the thin edge wedge could be possible. For instance, if the image displacement and the thin edge wedge are perpendicular the correlation fringes do not rotate but modify its spatial frequency. Indeed, as mentioned any relative displacement could be produced, but in this case the correlation fringes behavior is more complex.

It should be mentioned that the use of a parallel plate ($\tau = 0,\ \gamma \neq 0$) in the second exposure produces a uniform phase shift of the interference fringes with respect to the fringes obtained in the situation without phase object ($\tau = 0, \gamma = 0$) which does not affect the zero order and takes place in opposite directions in the lateral orders.

The detailed procedure constitutes the basis for implementing an alternative technique for phase object detection. It should be mentioned that wedge like phase objects with large enough phase variation could not be measured with the proposed technique as a consequence of the visibility behavior in those cases (see [12]). In summary, the technique is useful to determine very small angles concerning phase objects.

3. Soap film analysis set-up

In this section, the interferometer will be utilized to measure the thickness map of a vertical soap film. The optical set-up depicted in Fig. 1 is utilized. A diffuser is illuminated by a collimated He–Ne-laser beam and imaged onto the X–Y plane. A pupil mask with two square apertures is located in front of the imaging lens L. The square aperture has a side $D = 3.8$ mm and the aperture centers are separated by a distance $d = 10$ mm. The distances from the diffuser to the lens and from the lens to the image plane (X–Y plane) are $Z_0 = 135$ mm and $Z_C = 485$ mm, respectively. In the X–Y plane a CCD camera equipped with a zoom microscope is located to capture and afterwards to digitalize the image. The zoom-microscope provides a lateral magnification of $4.5\,X$ and is focused on the observation X–Y plane.

As a first step, an image speckle pattern obtained by using the arrangement shown in Fig. 1 is stored in a computer buffer memory. This is referred to as the reference speckle image. Afterwards, the soap film is placed in front of one aperture, a uniform diffuser in-plane displacement between exposures $(\Delta x^{12}, \Delta y^{12}) = (0\text{ mm}, 32 \times 10^{-3}\text{ mm})$ and a new dynamic speckle pattern is stored in the buffer memory. Note that the diffuser in-plane displacement Δy^{12} is done with a precision translation stage within 1 μm accuracy. In our experimental set-up, the soap film is produced by pulling a frame out of a reservoir solution. In this case, the drawing process takes place due to the drainage of the surfactant solution. As it was mentioned, the speckle images are transferred to the computer for processing and a sum of a given status of the speckle pattern and the reference speckle is done. The status of the soap film is determined by analyzing the correlation fringes obtained in real-time by applying a FFT algorithm to the resulting summed speckle image. This procedure is repeated as far as the soap film evolves in the successive status.

In Fig. 2 the diffraction pattern corresponding to different status of the soap film is displayed. The experiments have been carried out with aqueous solutions of sodium dodecyl sulphate. As mentioned in Section 2, the theoretical model predicts that if the diffuser in-plane displacement and the thin edge of the wedge are parallel, the correlation fringes direction rotates with respect to the situation without the wedge. The fringes rotation found in our experimental arrangement coincides with the behavior detailed. Therefore, this result allows to confirm that the soap film behaves as a wedge shaped film whose thin edge lies in Y-direction and it is parallel to the diffuser in-plane displacement. This result is reasonable by taking into account the gravity and capillarity effects. The thinning process in vertical soap film is due to the pressure difference between the film center and borders, caused by gravity and capillarity, acting in all cases. The borders of the film are curved to adjust the contact angle requirements with the supporting frame. As a consequence, the film is thicker at the borders and the pressure is smaller: this produces a sucking effect onto the liquid from the center to the borders [6]. Besides, note that we are observing only a portion

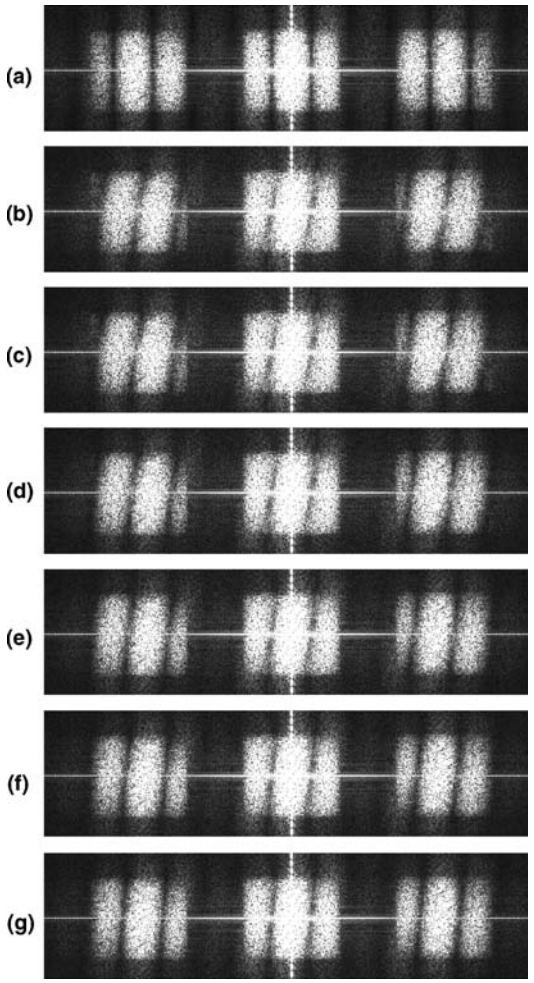

Fig. 2. Soap film evolution diffraction pattern.

of the soap film area because the pupil aperture is smaller than the supporting frame. In this sense, the observed region of the soap film is wedge shaped.

As detailed in the theoretical analysis, the phase changes that the soap film introduces to the aperture can be expressed as $\gamma + \tau u$. Besides, by determining the fringes orientation and position with respect to the reference correlation fringe image, the soap film parameters could be obtained. The reference correlation image corresponds to an in-plane displacement $\Delta y^{12} = 32 \times 10^{-3}$ mm and the absence of the soap film ($\tau = 0$, $\gamma = 0$) resulting in vertical correlation fringes (Fig. 2(a)). When the wedge shaped soap film is introduced, a fringes rotation with respect to the reference correlation fringes is observed (Fig. 2(b)–(g)). The angle between the correlation fringes and the vertical U-axis in the Fourier plane is given by $\alpha = \tan^{-1}\lfloor \lambda Z_C \tau / 4\pi \Delta Y^{12} \rfloor$ [12]. If in the soap film dynamic evolution a decreasing of the angle that forms the correlation fringes with the U-axis is observed, it implies that the parameter τ decreases. The experimental measurements of the parameters Z_0, Z_C, Δy^{12} and the angle α allow to determine the soap film parameter τ. The angles obtained from the experimental successive status of the soap film depicted in Fig. 2 are: $\alpha = 0$ in 2(a); $\alpha = 0.168$ rad in 2(b); $\alpha = 0.158$ rad in 2(c); $\alpha = 0.138$ rad in 2(d); $\alpha = 0.127$ rad in 2(e); $\alpha = 0.105$ rad in 2(f); and $\alpha = 0.085$ rad in 2(g). In this case, it results in: (a) $\tau = 0$ cm^{-1}; (b) $\tau = 8$ cm^{-1}; (c) $\tau = 7.5$ cm^{-1}; (d) $\tau = 6.5$ cm^{-1}; (e) $\tau = 6$ cm^{-1}; (f) $\tau = 5$ cm^{-1}; and (g) $\tau = 4$ cm^{-1}, respectively. Note that the dihedral angle that defines the soap film is $\beta = \tan^{-1}(\tau\lambda/(n-1)2\pi)$, where n is the soap film refractive index. Then, by considering $n = 1.333$, $\lambda = 633$ nm and the $|\tau|$ values determined above, the angle β results in: 50,37 arcsec in 2(b); 47,22 arcsec in 2(c); 40,93 arcsec in 2(d); 37,78 arcsec in 2(e); 31,48 arcsec in 2(f); and 25,18 arcsec in 2(g), respectively.

Note that additional information can be obtained. Remember that the wedge-like phase object in the theoretical model is governed by $\gamma + \tau u$ where the sign of the parameters must be considered. In Fig. 3, the diffraction order theoretical simulations corresponding to: (a) $\gamma = 0$, $\tau = 600\frac{1}{m}$; (b) $\gamma = 0$, $\tau = 0\frac{1}{m}$; and (c) $\gamma = 0$, $\tau = -600\frac{1}{m}$ are displayed. The theoretical simulation is computed by use of Eqs. (3) and (4) and by considering the parameters mentioned in Fig. 2. Note that in Fig. 3(a) the fringes are rotated with respect to the vertical U-axis in the same magnitude as in Fig. 3(c) but with different orientation. This distinct behavior of the fringes indicates whether the thicker part of the wedge is in the upper or lower region of the aperture. This feature allows to determine the slope sign (up or down orientation) of the soap film like wedge simply by observing the rotation direction. The results of Fig. 2 allow to assure that the soap film part analyzed is thicker in the upper region.

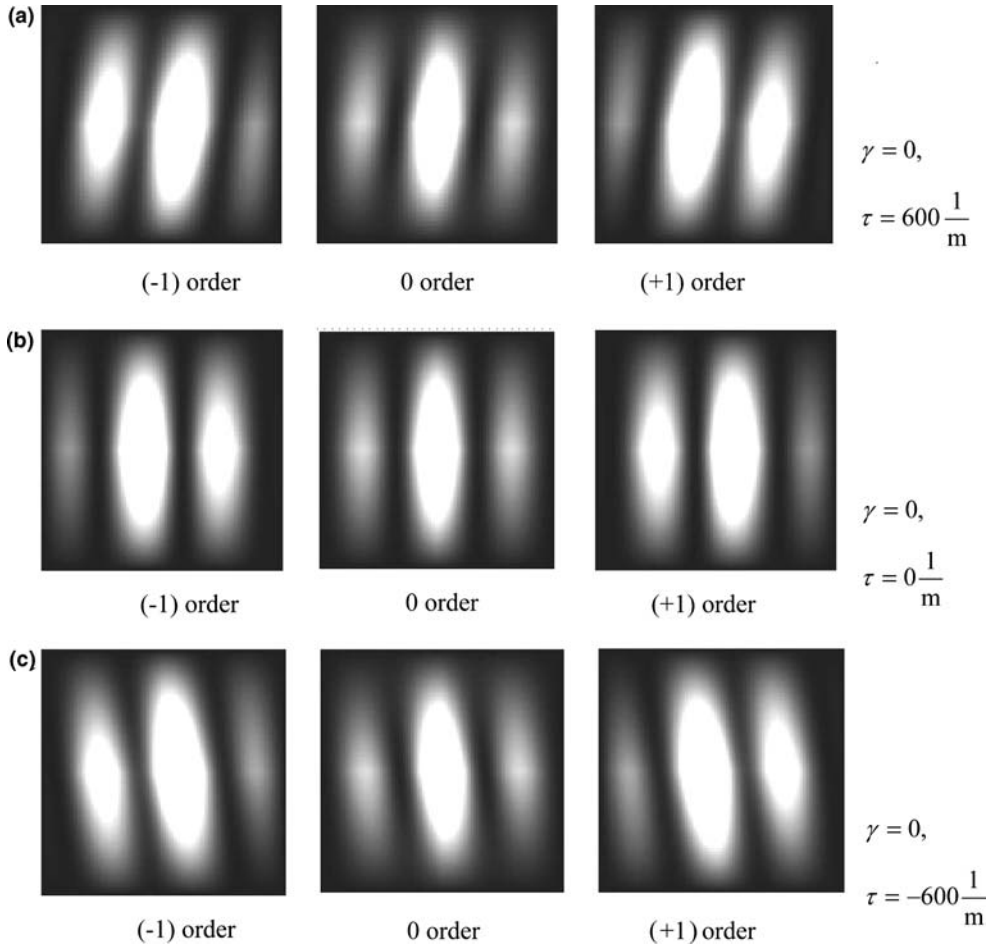

Fig. 3. Diffraction orders theoretical simulation which corresponds to: (a) $\gamma = 0,\ \tau = 600\frac{1}{m}$; (b) $\gamma = 0, \tau = 0\frac{1}{m}$; and (c) $\gamma = 0,$ $\tau = -600\frac{1}{m}$.

The determination of the parameter τ requires the accurate measurement of: the diffuser in-plane displacement Δy^{12}, the distances Z_0, Z_C and the correlation fringes orientation α. In our case, the accuracy is $\varepsilon(\Delta y^{12}) = 1$ μm, $\varepsilon(Z_0) = 0.5$ mm and $\varepsilon(Z_C) = 0.5$ mm. The relative errors are 1% and 0,1%, respectively. Concerning the interference fringes, an accurate determination of their orientation is required. An extensive review of techniques devoted to evaluate the interference fringes can be found in [15]. Main errors in fringes evaluation arise from speckle noise, which is inherent to the technique proposed. Computed based algorithms are used to an accurate measurement of the fringes orientation [16]. Taking into account all the source errors mentioned, we observed discrepancies below 2% in the determination of the soap film parameter τ.

It should be pointed out that to provide reliable information, the fringe pattern visibility must be higher than 0.5, otherwise the fringes analysis procedure fails. In summary, a correct processing of the correlation fringes and therefore an accurate measurement of the angle α will depend on the visibility behavior. As it was analyzed in [12], the fringe visibility at the central point of each diffracted order depends on D and τ values and is given by

$$\mathbf{V}^{\pm 1}(\mp d') = \frac{2t}{1+t^2}\,|\mathrm{sinc}(D\tau/2\pi)|,$$

where $d' \equiv fd/Z_C$. By considering the parameter of our experimental arrangement $D = 3.8$ mm, $t = 1$ and $|\tau| < 800\ \mathrm{m}^{-1}$, the visibility theoretically obtained is higher than 0.96, as can be confirmed by observing Fig. 2.

Also, the phase changes the soap film introduces to the aperture depends on the γ parameter values. As mentioned in Section 2, the use of a parallel plate ($\tau = 0$, $\gamma \neq 0$) in the second exposure produces a uniform phase shift of the interference fringes with respect to the fringes obtained in the situation without phase object ($\tau = 0, \gamma = 0$) which does not affect the zero order and takes place in opposite directions in the lateral orders. Let us observe in Fig. 4(a) theoretical simulations of the (-1) lateral diffraction order ($\tau = 0, \gamma \neq 0$) that corresponds to increasing values of the parameter γ. The theoretical simulation is computed by use of Eq. (4) and by considering the parameters mentioned in Fig. 2. It is clear that the fringes shift to the left, whereas Fig. 4(b) shows a (-1) lateral order ($\tau = 0, \gamma \neq 0$) that corresponds to decreasing values of the parameter γ and the fringes shift to the right. Then, in successive status of the soap film that will correspond to successive different

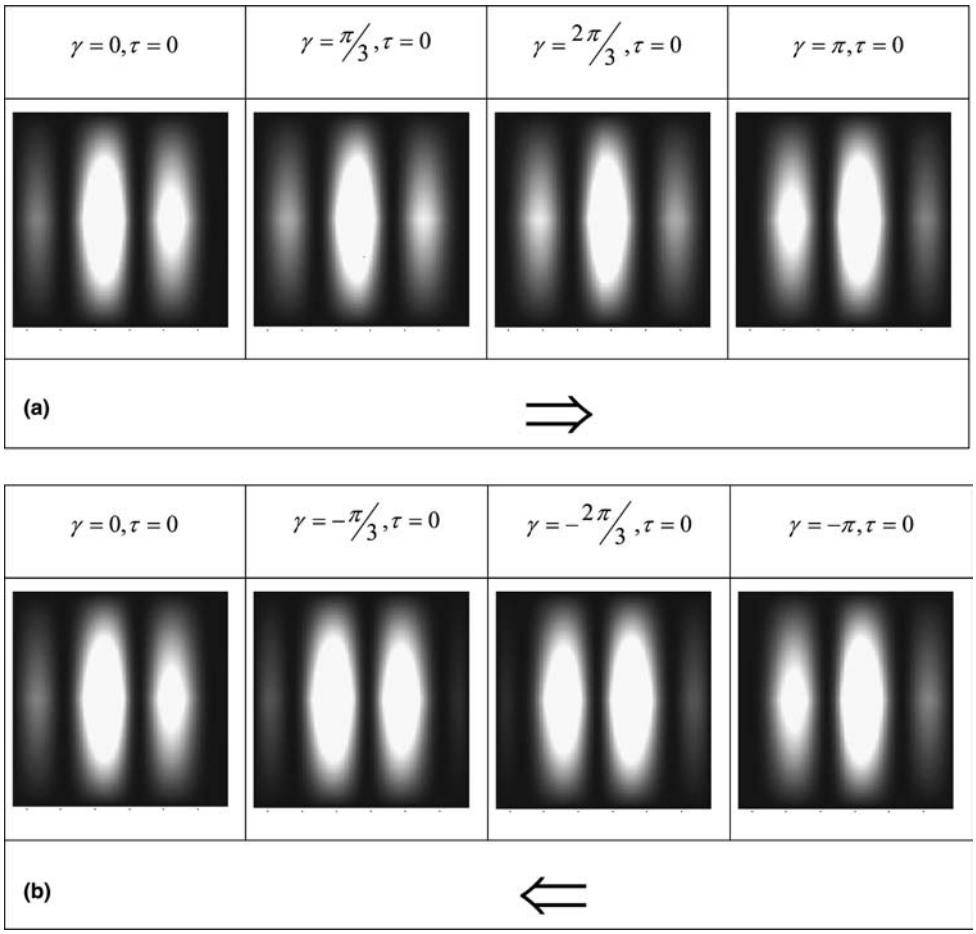

Fig. 4. (-1) lateral order theoretical simulation which corresponds to $\tau = 0$ and: (a) increasing values of γ ($\gamma = 0, \gamma = \pi/3, \gamma = 2\pi/3, \gamma = \pi$) and (b) decreasing values of γ ($\gamma = 0, \gamma = -\pi/3, \gamma = -2\pi/3, \gamma = -\pi$).

values of γ, the lateral fringes shift direction in that order will establish the thickness variation of the film between those successive status.

In our experimental condition (wedge shaped soap film with $\tau \neq 0$, $\gamma \neq 0$), the mentioned fringes shift in the lateral order is produced. After the determination of the parameter τ, it is necessary to measure this shift in for instance the (-1) lateral order to determine the parameter γ. Whereas to assess the parameter τ, the fringes correlation orientation must be obtained, the precise determination of the parameter γ depends on the successful measurement of the interference fringes profile to determine the mentioned fringes shift. As in the case of the parameter τ, a source error in the determination of γ arises from the speckle noise. It is clear that the ultimate resolution of the correlation fringes are limited by the speckle size which implies a limit to the pupil size. Computed based algorithms are used to measure the peak position [17,18]. Note that to obtain fringes that can be further processed by the computer, their thickness must be several times the diameter of a speckle grain because the noise that these grains introduce. In our case, a low pass filtering operation is applied to reduce the speckle noise. To apply the mentioned method, the fringes must be in vertical direction. The technique described in [16] to find the fringes inclination is utilized. Also, software procedure is used to rotate the image, so that the vertical condition can be achieved. Then, the peak position fringe evaluation allows to determine the (-1) lateral order fringes shift between successive status of the film and the parameter γ corresponding to the images showed in Fig. 2 results in: (b) $\gamma = 1.33\pi$; (c) $\gamma = 1.55\pi$; (d) $\gamma = 1.91\pi$; (e) $\gamma = 0.19\pi$; (f) $\gamma = 0.51\pi$; and (g) $\gamma = 0.76\pi$, respectively. In the results of Fig. 2, the fringes shifting direction, in the (-1) lateral order indicates that during drawing the soap film becomes thinner (thickness decreasing). Clearly, the same information can be obtained from the $(+1)$ lateral order. Discrepancies below 3% in the determination of the γ soap film parameter are observed. Notice that the quantity gamma is only determined modulus 2π which implies that the absolute value of the thickness is not possible to obtain. Nevertheless, this is not essential to monitor the evolution of the film thickness. Furthermore, in our experimental conditions the changes between successive status are much lesser than 2π.

As mentioned above, in our case the soap film is produced by pulling a frame out of a reservoir solution. The soap film during drawing acts as a variable wedge. The film behavior is due to the pressure difference between the film center and borders, caused both by gravity and capillarity. Indeed, the film is thicker at the borders as it is confirmed with our experimental results. This fact is due to a sucking effect onto the liquid from the center to the borders. The film becomes thinner as the drying process takes place as can be confirmed by the behavior of the parameter γ. Also, the wedge shaped film angle decreases while the film evolves. In this way, in accordance with the successive rotations of the fringes, the status of the film can be assessed.

4. Conclusions

A novel and simple speckle interferometric technique for characterizing vertical soap film is presented. The soap film is produced by pulling a frame out of a reservoir solution. The film thinning process is due to the pressure difference between the film center and borders, caused both by gravity and capillarity. The proposed method allows to monitor and to map the soap film as a function of the changes in the correlation fringes. In particular, the tilted fringes behavior observed with the soap film introduction, makes it possible to establish that the film during the drawing process acts as a variable wedge shaped film and also that the thin edge of the film and the diffuser in-plane displacement are parallel. Moreover, the fringe rotation direction with respect to the fringes orientation obtained without the introduction of the phase object permits to determine that the film is thicker at the borders and which border is thicker. Note that the proposed technique allows to establish whether the thicker part of the wedge is in the upper or lower region of the aperture. This feature is in accordance with the predictable sucking effect onto the liquid from the center to the borders. In fact, the technique could be used to determine the slope in the soap film boundary as well

as to measure the soap film thickness, in particular at the rupture time. Besides, in successive status of the soap film that will correspond to successive variation of the soap film parameters, the lateral fringes shift direction in the lateral diffraction order will establish the increasing or decreasing of the film thickness. In summary, the behavior of the fringes (direction rotation and shifting) became an important tool to determine the slope and the thickness variation of the soap film.

The fringe visibility depends on the soap film parameters. In particular, the technique is useful for characterizing very small angles concerning phase objects like the soap film analyzed. As it is usual in interferometric methods, the measured physical quantities, in our case the soap film parameters, are encoded in the high visibility fringe patterns. Afterwards, conventional techniques for fringe analysis are used to extract the information from the interferometric pattern.

Acknowledgements

This research was performed under the auspicious of CONICET, CICPBA, Fundación Antorchas, Faculty of Engineering of the National University of La Plata (Argentina). M. Trivi acknowledges helpful discussion to G. Molesini and the financial support of ICTP-TRIAL Programm, Trieste, Italia.

References

[1] I. Newton, Optics Book II, Part I, Smith and Watford, London, 1704.
[2] O. Bélorgey, J.J. Benattar, Phys. Rev. Lett. 66 (1991) 313.
[3] J. Leyklema, P.C. Scholten, K.J. Mysels, J. Chem. 69 (1965) 116.
[4] V. Greco, C. Iemmi, S. Ledesma, G. Molesini, G.P. Puccioni, F. Quercioli, Meas. Sci. Technol. 5 (1994) 900.
[5] V. Greco, G. Molesini, Meas. Sci. Technol. 7 (1996) 96.
[6] A.A. Sonin, A. Bonfillon, D. Langevin, J. Colloid Interf. Sci. 162 (1994) 323.
[7] M. Françon, in: J.C. Dainty (Ed.), Laser Speckle and Related Phenomena, Springer-Verlag, Berlin, 1975.
[8] D. Duffy, Appl. Opt. 11 (1972) 1778.
[9] L. Angel, M. Tebaldi, N. Bolognini, M. Trivi, J. Opt. Soc. Am. A 17 (2000) 107.
[10] L. Angel, M. Tebaldi, M. Trivi, N. Bolognini, J. Mod. Opt. 43 (2001) 1749.
[11] L. Angel, M. Tebaldi, M. Trivi, N. Bolognini, Opt. Lett. 27 (2002) 506.
[12] M. Tebaldi, L. Angel, M. Trivi, N. Bolognini, J. Opt. Soc. Am. A 20 (2003) 116.
[13] L.G. Blows, L.H. Tanner, J. Phys. E: Sci. Instrum. 7 (1974) 402.
[14] O. Kafri, Opt. Lett. 5 (1980) 555.
[15] N. Halliwell, C. Pickering, in: D. Robinson, G.T. Reid (Eds.), Interferogram Analysis. Digital Fringe Pattern Measurement Techniques, Institute of Physics Publishing, 1993, p. 230.
[16] D. Robinson, Appl. Opt. 22 (1983) 2169.
[17] J. Pomarico, R. Arizaga, R. Torroba, H. Rabal, Optik 95 (1994) 125.
[18] J.H. Yi, S.J. Kim, I.K. Kwak, Y.W. Lee, Opt. Eng. 41 (2002) 428.